Models and Algorithms for Thin-Walled Structures in the 2020s

Antti H. Niemi, University of Oulu, Finland

Tampere University Visiting Lecture, 27.08.2020

Curved shell structures: background

$$t = \frac{d}{R} \ll 1$$

Shell structures

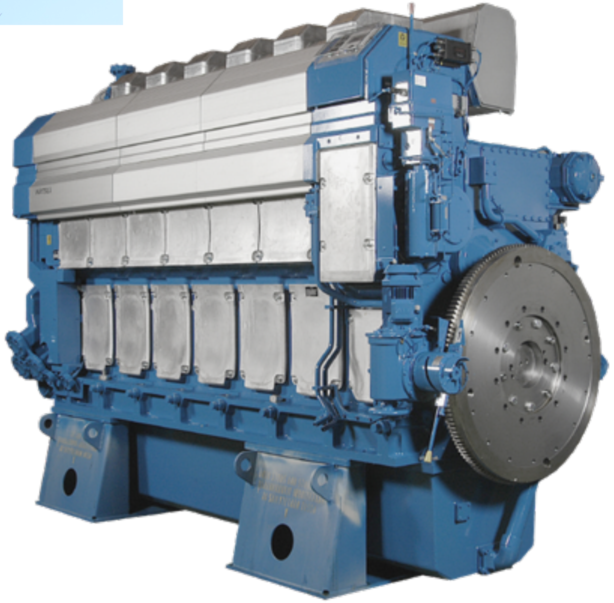

- Widely employed in civil and mechanical engineering
- Structural response of a shell can be very sensitive to disturbances in the geometry, material properties, boundary conditions, and loading.
- Shell is known as the *prima donna of structures* [Ekkehard Ramm]

Shell structures in civil engineering

Shell structures in civil engineering

Haukilahti water tower in Espoo

- Constructed in 1968 (3M FIM)
- Renovated between 2011-2012 (4.6M EUR)

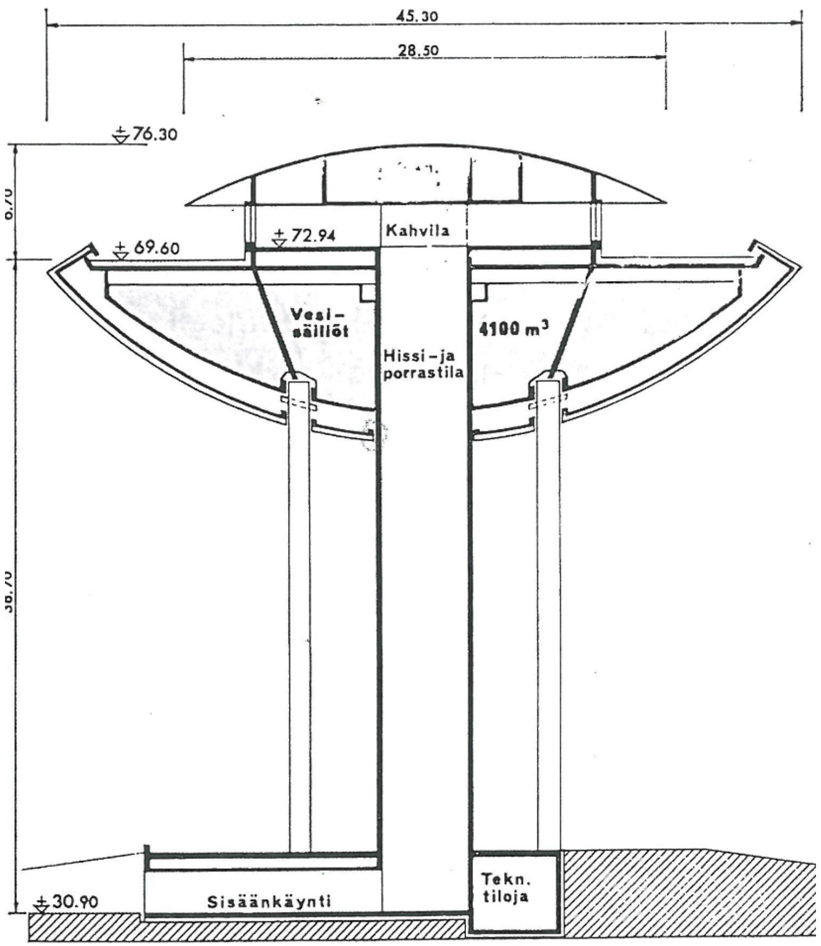

Original structural analysis

- Sophisticated application of plate and shell theory
- Linear algebraic equations with 10-20 unknowns
- Supercomputer was needed!

Different methods for thin shell analysis have their own benefits

- The theoretical rate of convergence of the *p*-type methods is superior
- The *h*-method has better sparsity properties
- Analytical methods could be applied in many relevant special cases

Mathematical shell models

Shell theory

"Shell theory attempts the impossible: to provide a two-dimensional representation of an intrinsically three-dimensional phenomenon."

[W. Koiter & J. Simmons]

- The models take the form

$$\mathcal{M}(\boldsymbol{u}) + t^2\mathcal{B}(\boldsymbol{u}) = \boldsymbol{f} \quad \text{on } \Omega \subset \mathbb{R}^2$$

- Tensor calculus may be used in the general description

Circular cylindrical shell geometry

Midsurface $\Omega \subset \mathbb{R}^2$
parametrized using
distance-measuring
coordinates x, y

Thickness $d \ll R$

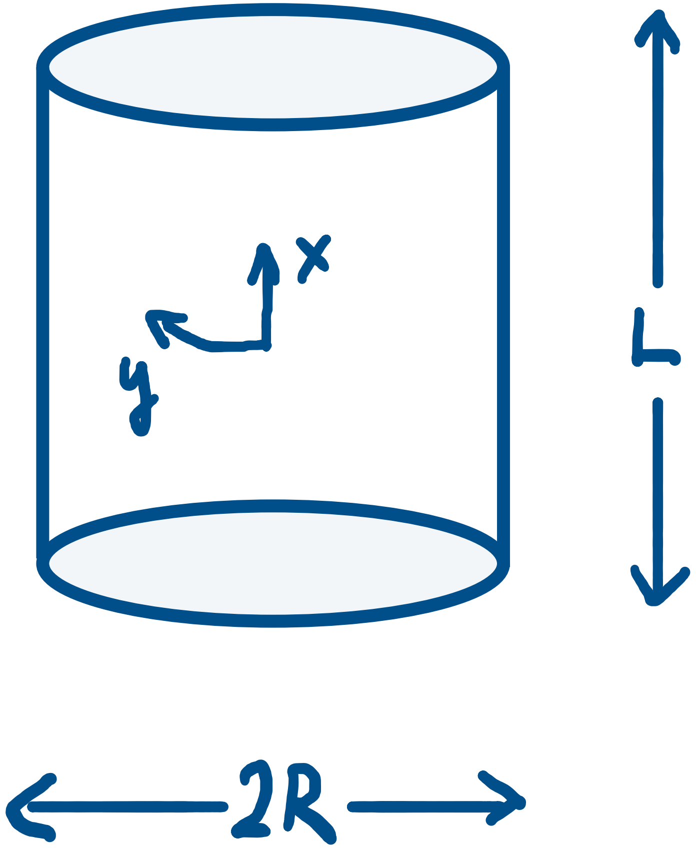

Displacement field

Displacement field defined on Ω:

$U = (u_x, u_y, w)$ or $U = (u_x, u_y, w, \theta_x, \theta_y)$

u_x, u_y – tangential displacements

w – transverse deflection

θ_x, θ_y – optional rotations

Strain energy product

Love - Novozhilov - Koiter (LNK):

$$A(U,V) = A_m(U,V) + A_b(U,V)$$

Reissner - Naghdi (RN):

$$A(U,V) = A_m(U,V) + A_s(U,V) + A_b(U,V)$$

Bilinear forms (cont.)

$$A_m(U,V) = \int_\Omega C_m\, B(U) : B(V)\, dxdy$$

$$A_b(U,V) = \int_\Omega C_b\, K(U) : K(V)\, dxdy$$

$$A_s(U,V) = \int_\Omega C_s\, \gamma(U) \cdot \gamma(V)\, dxdy$$

Kinematics

Membrane strains:

$$\beta_{xx} = \frac{\partial u_x}{\partial x}, \quad \beta_{yy} = \frac{\partial u_y}{\partial y} + \frac{w}{R}, \quad \beta_{xy} = \frac{1}{2}\left(\frac{\partial u_x}{\partial y} + \frac{\partial u_y}{\partial x}\right)$$

Bending curvatures:

$$K_{xx} = \frac{\partial \theta_x}{\partial x}, \quad K_{yy} = \frac{\partial \theta_y}{\partial y}, \quad K_{xy} = \frac{1}{2}\left(\frac{\partial \theta_x}{\partial y} + \frac{\partial \theta_y}{\partial x} + \frac{1}{R}\frac{\partial u_y}{\partial x}\right)$$

Kinematics (cont.)

Optional transverse shear strains:

$$\gamma_x = \theta_x + \frac{\partial w}{\partial x}, \quad \gamma_y = \theta_y + \frac{\partial w}{\partial y} - \frac{u_y}{R}$$

LNK model: $\gamma_x = \gamma_y = 0 \Rightarrow \kappa = \kappa(u_x, u_y, w)$

Constitutive law

Plane stress constitutive law for homogeneous and isotropic material (E, ν):

$$C\varepsilon = \frac{E}{1-\nu^2}\left[\nu\, tr(\varepsilon) I + (1-\nu)\varepsilon\right]$$

We have

$$C_m = d \cdot C, \quad C_b = \frac{d^3}{12} \cdot C, \quad C_s = d \cdot \frac{E}{2(1+\nu)}$$

Energy spaces

Energy space:

$$\mathcal{U} = \{ v \text{ kinematically admissible} : A(v,v) < \infty \}$$

RN: $\mathcal{U} \subset [H^1(\Omega)]^5$

LNK: $\mathcal{U} \subset H^1(\Omega) \times H^1(\Omega) \times H^2(\Omega)$

Shell Elements

State of the art

Shell FEM – High Order?

Computational efficiency is a function of many factors such as:

- Model Preparation, Adaptivity and Quality Control (*Simulation Governance* according to Szabo and Actis)
- Conditioning
- Distortion Sensitivity
- Locking

Shell Elements

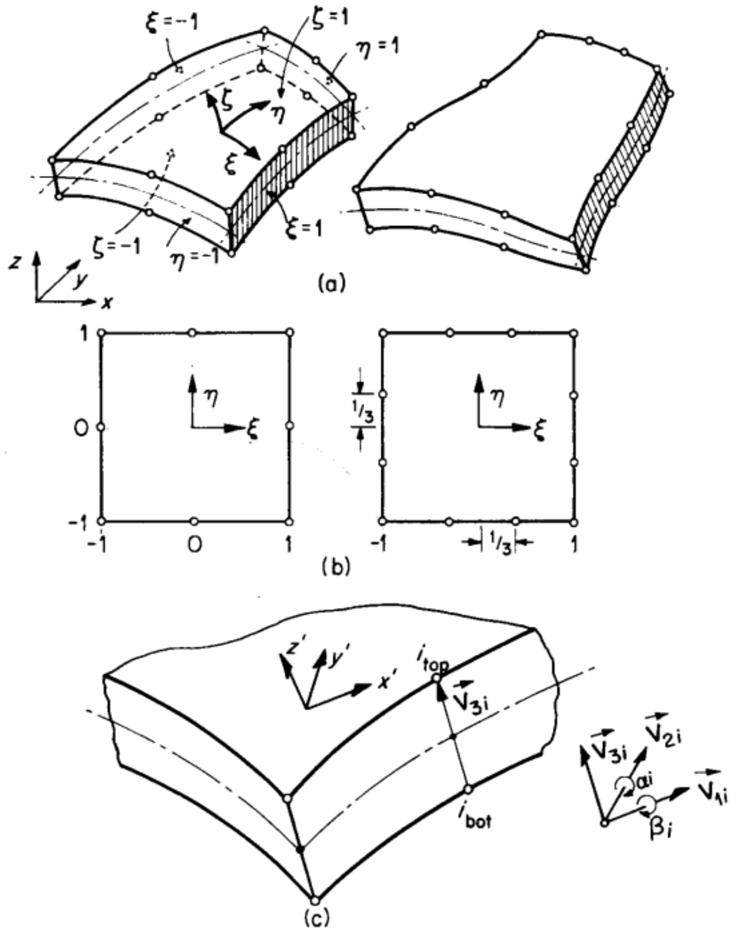

1970: Analysis of thick and thin shell structures by curved finite elements (Ahmad, Irons & Zienkiewicz, IJNME)

1978: A simple quadrilateral shell element (Macneal, COMPUT STRUCT)

1986: A formulation of general shell elements – the use of mixed interpolation of tensorial components (Bathe & Dvorkin, IJNME)

Convergence Theory of Shell Elements

$$e_a \leq C_1 h|\mathbf{u}_0|_2 + C_2 h^{2/3(s-1)}|\mathbf{u}_0|_s, \quad 2 \leq s \leq 3$$

$$e_c \leq C_1 h|\mathbf{u}|_2 + C_2 t^{-1} h^{s-1}|\mathbf{u}|_s, \quad s \geq 2$$

$$e_a \sim \left(\frac{R}{t}\right)^{1/3} h_x + h_y$$

$$e_c \sim h_x + \left(\frac{R}{t}\right)^{1/2} h_y.$$

1992: The problem of membrane locking in finite element analysis of cylindrical shells (Pitkäranta, NUMER. MATH.)

2002-2003: Analysis of a bilinear finite element for shallow shells I & II (Havu & Pitkäranta, MATH. COMPUT.)

2008: Approximation of shell layers using bilinear elements on anisotropically refined meshes (Niemi, CMAME)

Shell Elements Revisited

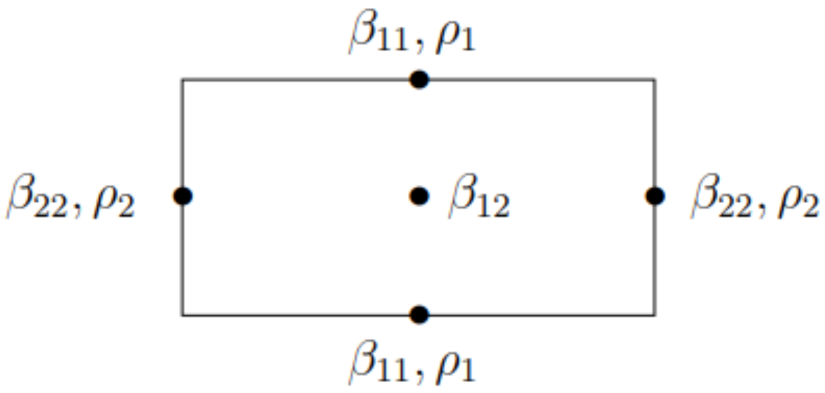

2010: A bilinear shell based on a refined shallow shell model (Niemi, IJNME)

2014: The MITC3+ shell element and its performance (Lee, Lee & Bathe, COMPUT STRUCT)

2016: The MITC4+ shell element and its performance (Ko, Lee & Bathe, COMPUT STRUCT)

2017: A new MITC4+ shell element (Ko, Lee & Bathe, COMPUT STRUCT)

Shell Kinematics

- **Kinematic hypothesis:**

$$\vec{U}(x,y,\zeta) = (u_\lambda(x,y) + \zeta\theta_\lambda(x,y))\vec{e}^{\lambda}(x,y) + w(x,y)\vec{n}(x,y),$$

where
$\boldsymbol{u} = (u_1, u_2)$ **are the tangential displacements**
w **is the transverse deflection**
$\boldsymbol{\theta} = (\theta_1, \theta_2)$ **are the angles of rotation of the normal**

- **Here** x, y **are coordinates used to parametrize the mid-surface and** ζ **the coordinate along its normal** $\vec{n}(x,y)$

Local shell coordinates

- **Assume that the shell mid-surface is discretized using triangular/quadrilateral elements**
- **(*x*,*y*) are some chosen Cartesian coordinates on each element *K***

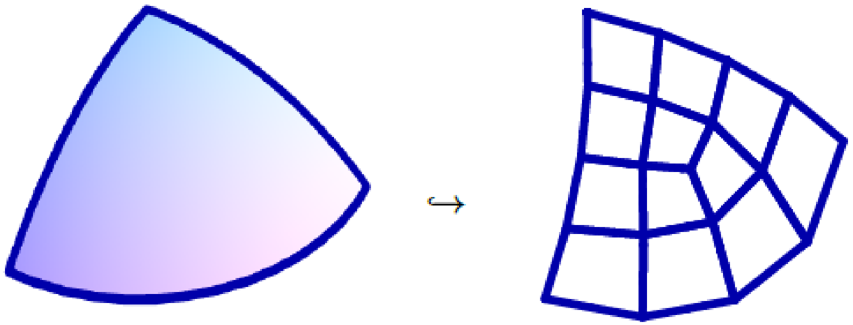

- **The (reasonable) meshing assumption is that each K is so small that x, y, ζ can be assumed *orthogonal* on K**

Global shell coordinates

Assume that the mid-surface is described by a chart $\boldsymbol{r}(x, y)$ and discretize in the parametric domain:

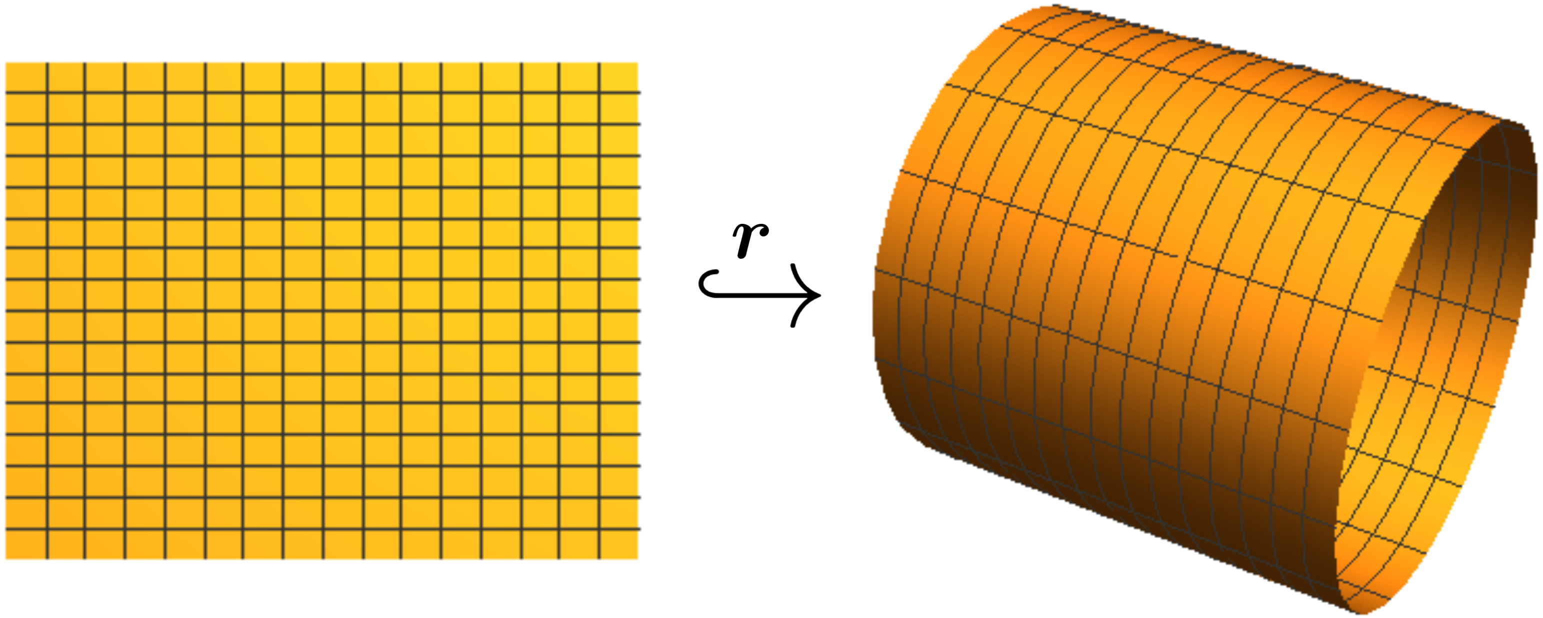

Curvilinear Strains

- **In-plane Green-Lagrange strain tensor:**

$$e_{\alpha\beta} \overset{d/R \ll 1}{\approx} \varepsilon_{\alpha\beta} + \zeta\kappa_{\alpha\beta}, \quad \alpha,\beta = 1,2.$$

- **The *membrane strain tensor* can be written as**

$$\varepsilon_{\alpha\beta} = \frac{1}{2}(u_{\alpha|\beta} + u_{\beta|\alpha}) - b_{\alpha\beta}w \overset{h/R \ll 1}{\approx} \frac{1}{2}(u_{\alpha,\beta} + u_{\beta,\alpha}) - b_{\alpha\beta}w,$$

where

$$b_{\alpha\beta} = -\vec{e}_\alpha \cdot \vec{n}_{,\beta}, \quad \alpha,\beta = 1,2,$$

is the second fundamental form of the mid-surface.

Curvilinear Strains

- **Introducing the third fundamental form**

$$c_{\alpha\beta} = \vec{n}_{,\alpha} \cdot \vec{n}_{,\beta}, \quad \alpha, \beta = 1, 2,$$

  the elastic curvature tensor comes out as

$$\kappa_{\alpha\beta} = \frac{1}{2}(\theta_{\alpha|\beta} + \theta_{\beta|\alpha}) + c_{\alpha\beta} w - \frac{1}{2}(b^{\lambda}_{\alpha} u_{\lambda|\beta} + b^{\lambda}_{\beta} u_{\lambda|\alpha}), \quad \alpha, \beta = 1, 2$$

- **Because** $c_{\alpha\beta} \overset{h}{\approx} b_{\alpha\lambda} b_{\lambda\beta}$ **, it is possible to write**

$$\kappa_{11} \overset{h}{\approx} \underline{\theta_{1,1} + b_{12}(b_{12} w - u_{2,1})} - b_{11}\varepsilon_{11},$$

$$\kappa_{22} \overset{h}{\approx} \underline{\theta_{2,2} + b_{12}(b_{12} w - u_{1,2})} - b_{22}\varepsilon_{22},$$

$$\kappa_{12} \overset{h}{\approx} \underline{\frac{1}{2}(\theta_{1,2} + \theta_{2,1}) + \frac{b_{11}}{2}(b_{12} w - u_{1,2}) + \frac{b_{22}}{2}(b_{12} w - u_{2,1})} - \frac{b_{12}}{2}(\varepsilon_{11} + \varepsilon_{22}).$$

Strain Energy Functional

- **Transverse shear strains:**

$$\gamma_\alpha = 2e_{\alpha 3} = \theta_\alpha + b_\alpha^\lambda u_\lambda + w_{,\alpha} \overset{h}{\approx} \theta_\alpha + b_{\alpha\lambda} u_\lambda + w_{,\alpha}$$

- **The strain energy functional:**

$$U_K(\boldsymbol{u}, w, \boldsymbol{\theta}) = \frac{1}{2} \int_K (n_{\alpha\beta}\varepsilon_{\alpha\beta} + q_\alpha \gamma_\alpha + m_{\alpha\beta}\kappa_{\alpha\beta})\, dS$$

- **Linearly elastic isotropic material (orthogonal coordinates):**

$$n_{\alpha\beta} = \frac{Ed}{1-\nu^2}\left[(1-\nu)\varepsilon_{\alpha\beta} + \nu\varepsilon_{\lambda\lambda}\delta_{\alpha\beta}\right],$$

$$q_\alpha = \frac{Ed}{2(1+\nu)}\gamma_\alpha,$$

$$m_{\alpha\beta} = \frac{Ed^3}{12(1-\nu^2)}\left[(1-\nu)\kappa_{\alpha\beta} + \nu\kappa_{\lambda\lambda}\delta_{\alpha\beta}\right]$$

Skew Coordinate Transformations

- Two orthogonal directions $\vec{g}_1, \vec{g}_2$ to the nodal normals are generated and a skew coordinate transformation

$$u_\alpha^K \circ T_K = \tilde{u}_\lambda \vec{g}_\lambda \cdot \vec{i}_\alpha, \quad w^K \circ T_K = \tilde{w}, \quad \theta_\alpha^K \circ T_K = \tilde{\theta}_\lambda \vec{g}_\lambda \cdot \vec{i}_\alpha.$$

is employed when enforcing the continuity of the displacements between elements.

- The geometric curvatures can be calculated from the interpolated normal vector $\vec{n}_h$ as

$$b_{\alpha\beta} \overset{h}{\approx} -\vec{i}_\alpha \cdot \vec{n}_{h,\beta}$$

Shear Locking (Plates)

- **The standard energy principle for the Reissner-Mindlin plate bending model gives raise to the constraint**

$$\boldsymbol{\theta} + \boldsymbol{\nabla} w = 0 \qquad (1)$$

which leads to locking if the FE space for $\boldsymbol{\theta} = (\theta_1, \theta_2)$ is too small.

- **Possible remedies:**

a) Use *hp*-method with *p* large enough

b) Replace $\boldsymbol{\theta} + \boldsymbol{\nabla} w = 0$ by $\boldsymbol{\Lambda}_h(\boldsymbol{\theta} + \boldsymbol{\nabla} w) = 0$ (mixed method)

c) Replace *t* by *h* in the shear energy term (penalty method)

Membrane and Shear Locking (Shells)

- ***Bending-dominated*** **deformations give raise to constraints**

$$\boldsymbol{\theta} + \mathbf{B}\mathbf{u} + \boldsymbol{\nabla} w = \mathbf{0} \tag{1}$$

$$\frac{1}{2}(\boldsymbol{\nabla}\mathbf{u} + \boldsymbol{\nabla}^{\mathrm{T}}\mathbf{u}) + \mathbf{B}w = \mathbf{0} \tag{2}$$

which lead to locking if the FE space for $(\boldsymbol{u}, w, \boldsymbol{\theta})$ **is too small**

- **Possible remedies:**

a) Use *hp*-method with *p* large enough

b) Replace (1) and (2) by

$$\boldsymbol{\Lambda}_h(\boldsymbol{\theta} + \mathbf{B}\boldsymbol{u} + \boldsymbol{\nabla} w) = \mathbf{0} \tag{1_h}$$

$$\boldsymbol{\Pi}_h\left(\frac{1}{2}(\boldsymbol{\nabla}\mathbf{u} + \boldsymbol{\nabla}^{\mathrm{T}}\mathbf{u}) + \mathbf{B}w\right) = \mathbf{0} \tag{2_h}$$

c) Replace *t* by *h* in the shear energy term (penalty method)

Displacement Approximations

- *h*-version: Linear approximation for each displacement component separately on each *K* (*Courant triangle*)

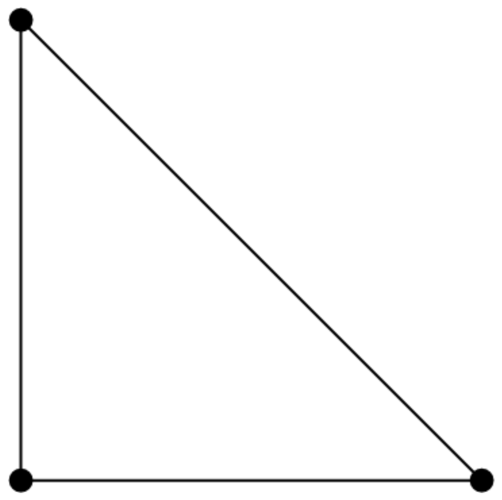

- *p*-version: Full tensor-product space on quads using *integrated Legendre polynomials (or NURBS)*

Strain reductions for the *h*-version

- Define on $\hat{K}$ the FE spaces

$$\boldsymbol{S}(\hat{K}) = \{\hat{\boldsymbol{s}} = \begin{pmatrix} a + c\hat{y} \\ b - c\hat{x} \end{pmatrix} \; : \; a,b,c \in \mathbb{R}\}$$

$$\boldsymbol{M}(\hat{K}) = \{\hat{\boldsymbol{\tau}} = \begin{pmatrix} a & b \\ b & c \end{pmatrix} \; : \; a,b,c \in \mathbb{R}\}$$

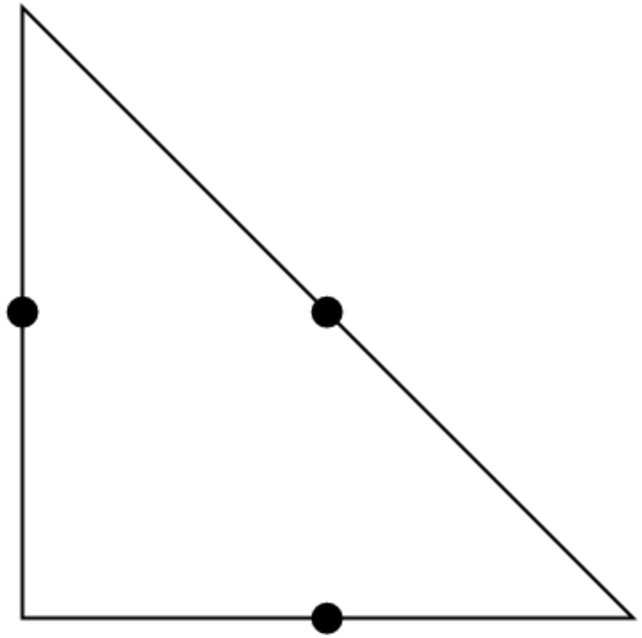

- The associated DOFs are

$$\hat{\boldsymbol{s}} \mapsto \int_{\hat{e}} \hat{\boldsymbol{s}}^T \hat{\boldsymbol{t}} \, d\hat{s} \text{ for every edge } \hat{e} \text{ of } \hat{K},$$

$$\hat{\boldsymbol{\tau}} \mapsto \int_{\hat{e}} \hat{\boldsymbol{t}}^T \hat{\boldsymbol{\tau}} \hat{\boldsymbol{t}} \, d\hat{s} \text{ for every edge } \hat{e} \text{ of } \hat{K}.$$

Strain reductions

- The corresponding spaces associated to a general *K* are

$$\boldsymbol{S}(K)=\{\boldsymbol{s}=\boldsymbol{J}_K^{-T}\hat{\boldsymbol{s}}\circ\boldsymbol{F}_K^{-1}=\mathcal{S}_K(\hat{\boldsymbol{s}})\;:\;\hat{\boldsymbol{s}}\in\boldsymbol{S}(\hat{K})\}$$
$$\boldsymbol{M}(K)=\{\boldsymbol{\tau}=\boldsymbol{J}_K^{-T}(\hat{\boldsymbol{\beta}}\circ\boldsymbol{F}_K^{-1})\boldsymbol{J}_K^{-1}=\mathcal{M}_K(\hat{\boldsymbol{\tau}})\;:\;\hat{\boldsymbol{\tau}}\in\boldsymbol{M}(\hat{K})\}$$

- The projectors are defined as

$$\boldsymbol{\Pi}_K=\mathcal{M}_K\circ\boldsymbol{\Pi}_{\hat{K}}\circ\mathcal{M}_K^{-1}\text{ and }\boldsymbol{\Lambda}_K=\mathcal{S}_K\circ\boldsymbol{\Lambda}_{\hat{K}}\circ\mathcal{S}_K^{-1}$$

where $\boldsymbol{\Lambda}_{\hat{K}}:\boldsymbol{H}^1(\hat{K})\to\boldsymbol{S}(\hat{K})$ and $\boldsymbol{\Pi}_{\hat{K}}:\boldsymbol{H}^1(\hat{K})\to\boldsymbol{M}(\hat{K})$ are well-defined

- The DOFs (tangential components) are preserved.

- **MITC3C:** $\gamma \hookrightarrow \Lambda_K \gamma$

- **MITC3S:** $\varepsilon \hookrightarrow \mathbf{\Pi}_K \varepsilon, \quad \gamma \hookrightarrow \Lambda_K \gamma$

- **Stabilized variants of both elements can be introduced by modifying the shear modulus as**

$$G \hookrightarrow G_K = \frac{t^2}{t^2 + \alpha_K h_K^2} \cdot G.$$

Linear Bar Approximation of an Arch on (-h/2,h/2)

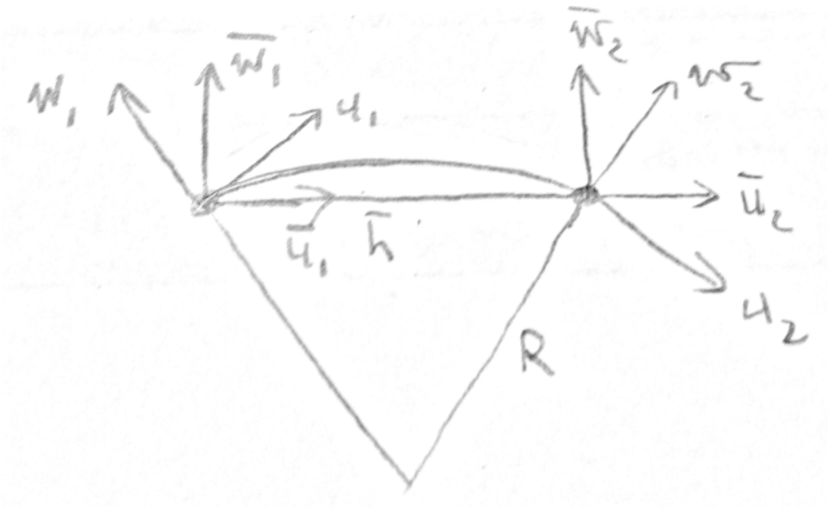

$$\bar{u}_2 = \cos\left(\frac{h}{2R}\right) u_2 + \sin\left(\frac{h}{2R}\right) w_2$$

$$\bar{u}_1 = \cos\left(\frac{h}{2R}\right) u_1 - \sin\left(\frac{h}{2R}\right) w_1$$

$$\bar{\beta}_{ss} = \frac{\bar{u}_2 - \bar{u}_1}{\bar{h}} = \frac{1}{\bar{h}}\left(\cos\left(\frac{h}{2R}\right)(u_2 - u_1) + \sin\left(\frac{h}{2R}\right)(w_1 + w_2)\right)$$

$$\approx \frac{u_2 - u_1}{h} + \frac{1}{2R}(w_1 + w_2) = \beta_{ss}(0) = u_h'(0) + \frac{w_h(0)}{R} = \pi\beta_{ss}$$

Regular triangulation of circular cylinder

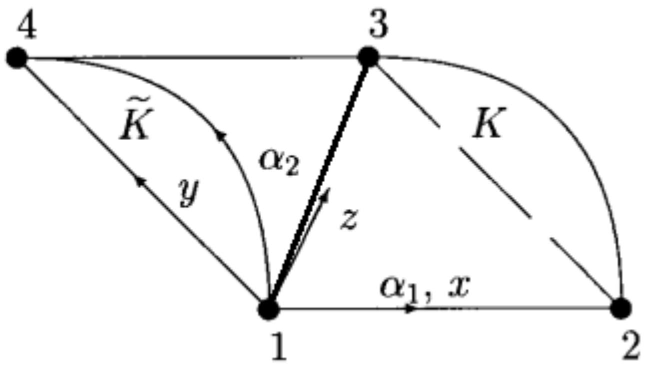

$$\beta_{11} = \frac{\partial u}{\partial \alpha_1}, \quad \beta_{22} = \frac{\partial v}{\partial \alpha_2} + \frac{w}{R}, \quad \beta_{12} = \frac{1}{2}\left(\frac{\partial u}{\partial \alpha_2} + \frac{\partial v}{\partial \alpha_1}\right)$$

$$\hookrightarrow \bar{\beta}_{11} = \pi_1 \beta_{11}, \quad \bar{\beta}_{22} = \pi_2 \beta_{22}, \quad \bar{\beta}_{12} = \pi_{12}\beta_{12} + \mathcal{O}(h_K^2)$$

Benchmark computations

Pitkäranta's Cylinder CMAME 128 (1995), pp. 81-121

– Cylindrical shell with half-length H = radius R:

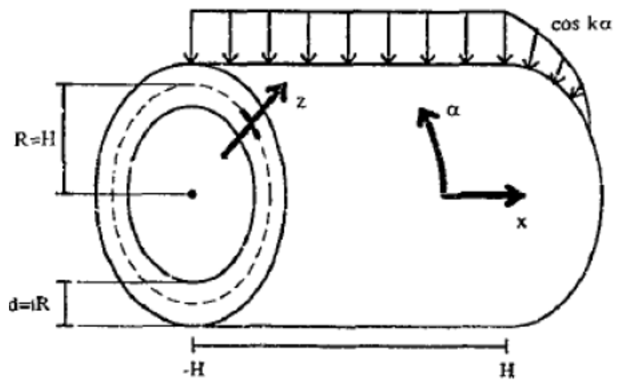

– Features all asymptotic categories of shell deformations:

1. Clamped ends -> Membrane-dominated
2. Free ends -> Bending-dominated
3. Simply supported ends -> Intermediate state (edge effect dominates)

Meshes

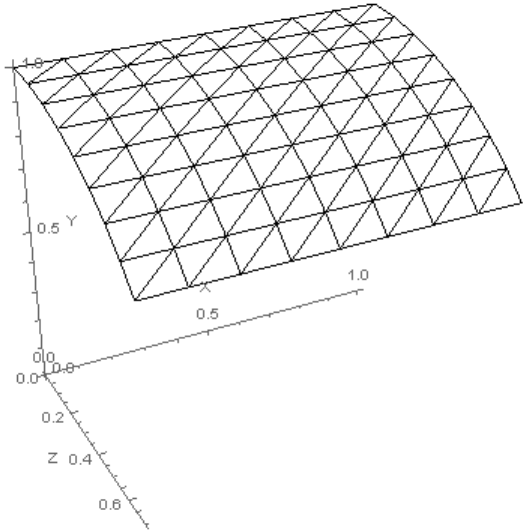

Uniform

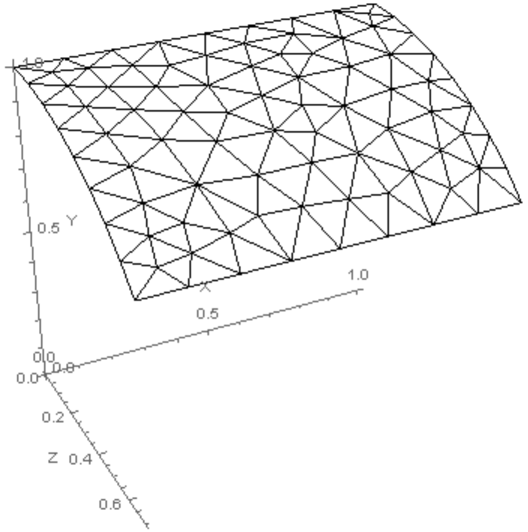

Delaunay

Error Indicator

- ***Strain energy error indicator:***

$$e(h) = \sqrt{\frac{|U_{\text{ref}} - U_h|}{U_{\text{ref}}}}, \quad h = \frac{1}{N}$$

- **Not completely reliable for non-conforming FE methods, but error computation is straightforward**

- **Ideally, $e(h)$ should not depend on the ratio R/t**

Circular cylinder with free ends (COMSOL)

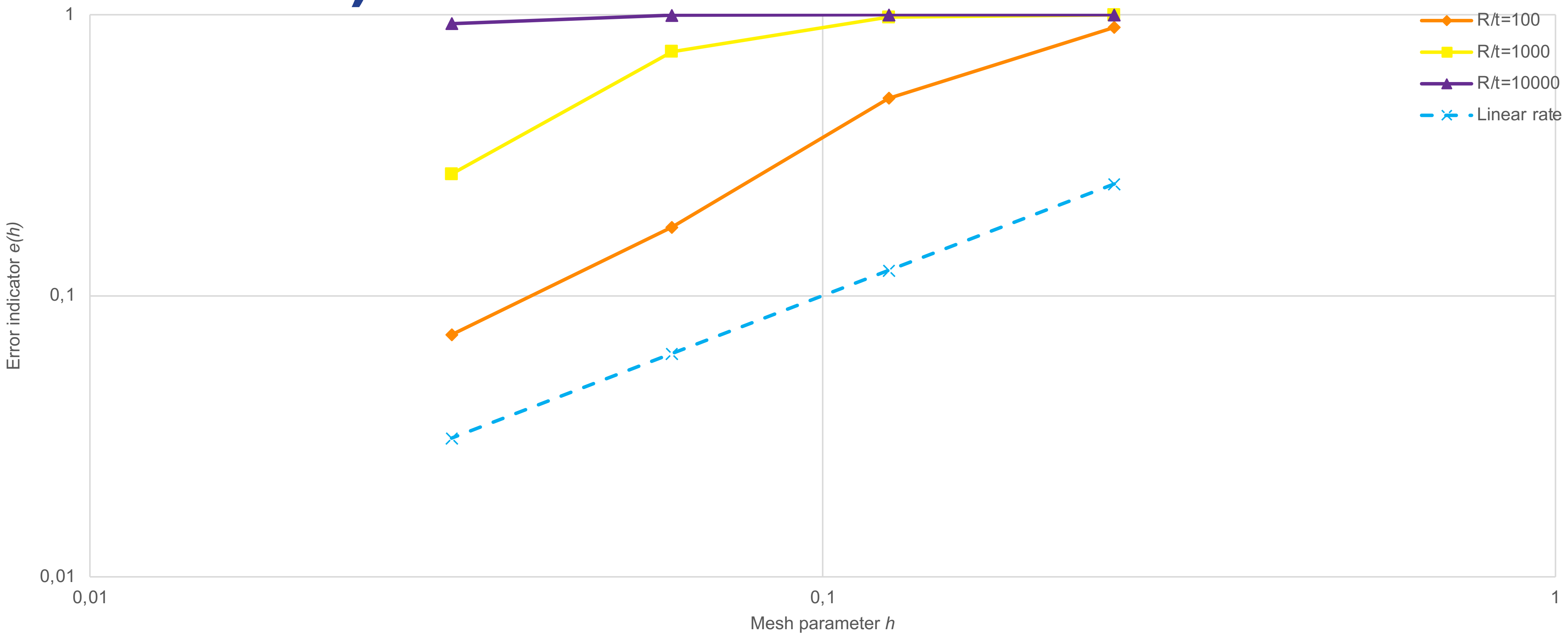

Circular cylinder with free ends MITC3S (Delaunay)

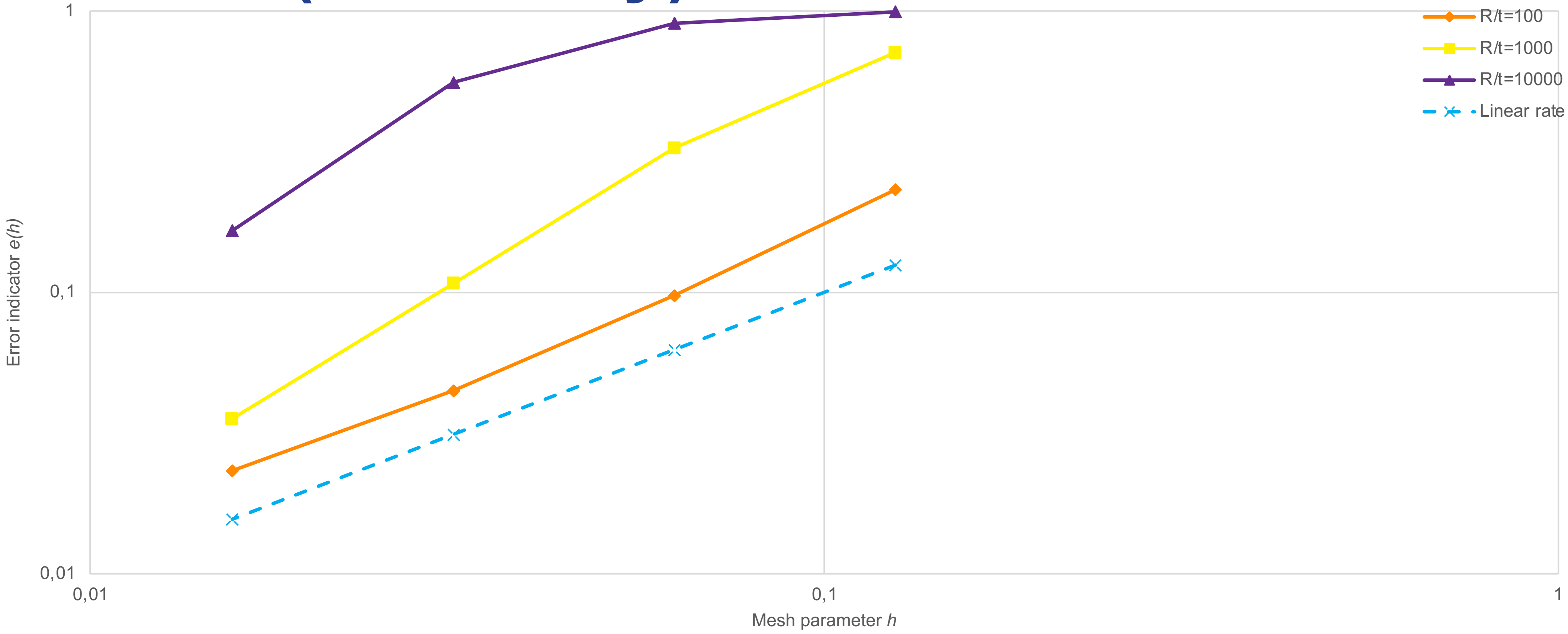

Circular cylinder with free ends Stabilized MITC3S (Delaunay)

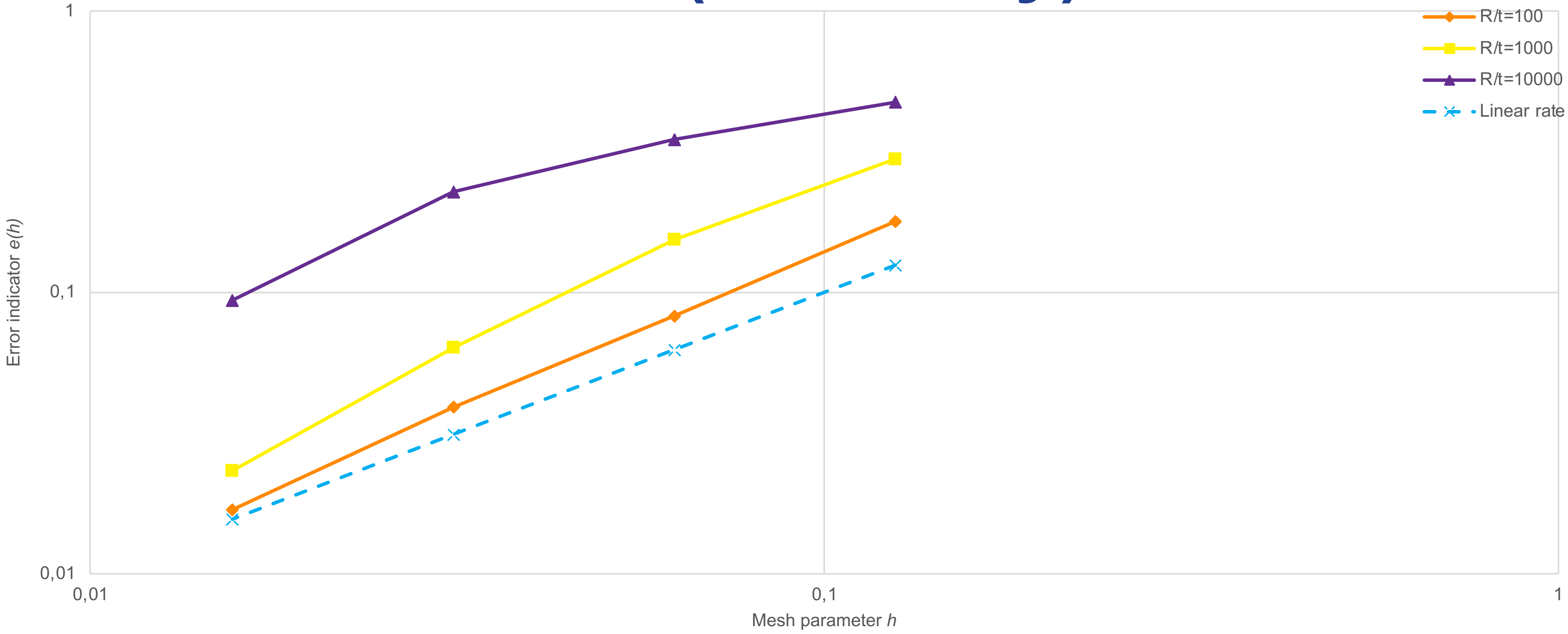

Circular cylinder with free ends MITC3S (uniform)

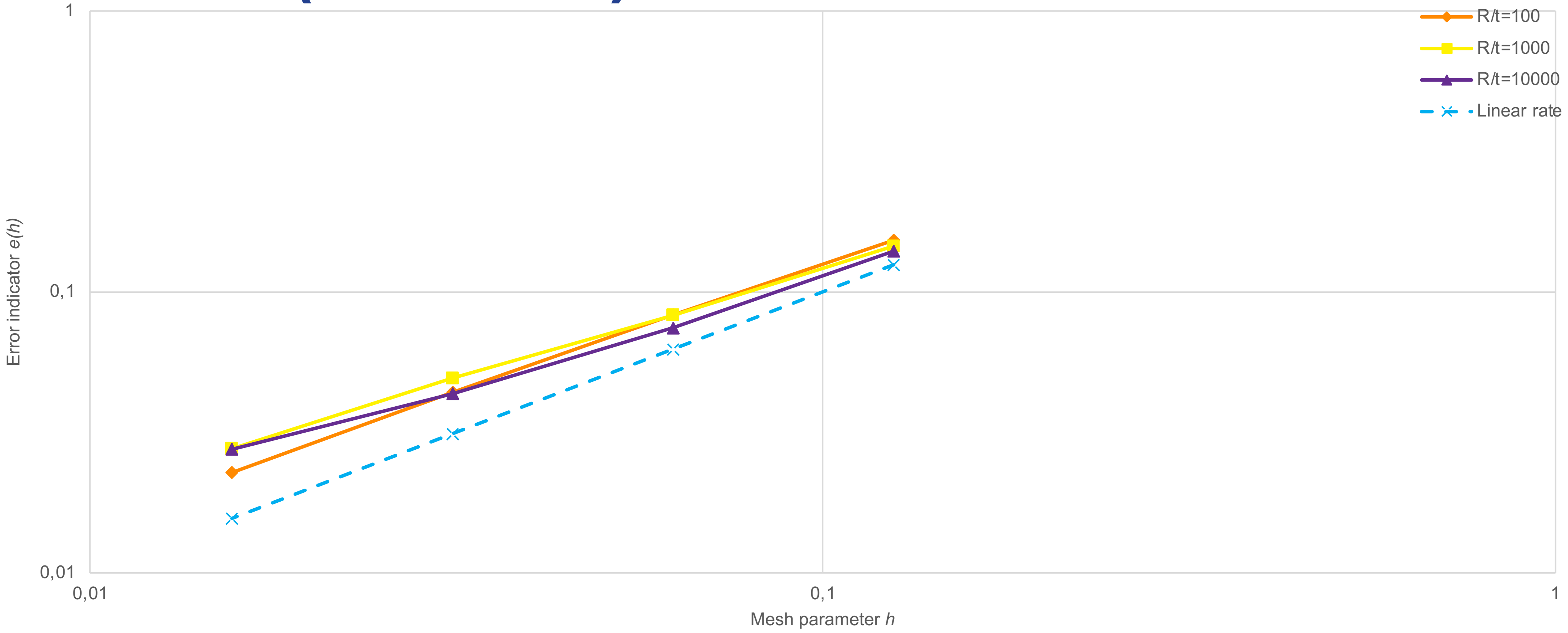

Circular Cylinder with Clamped Ends Stabilized MITC3C (Delaunay)

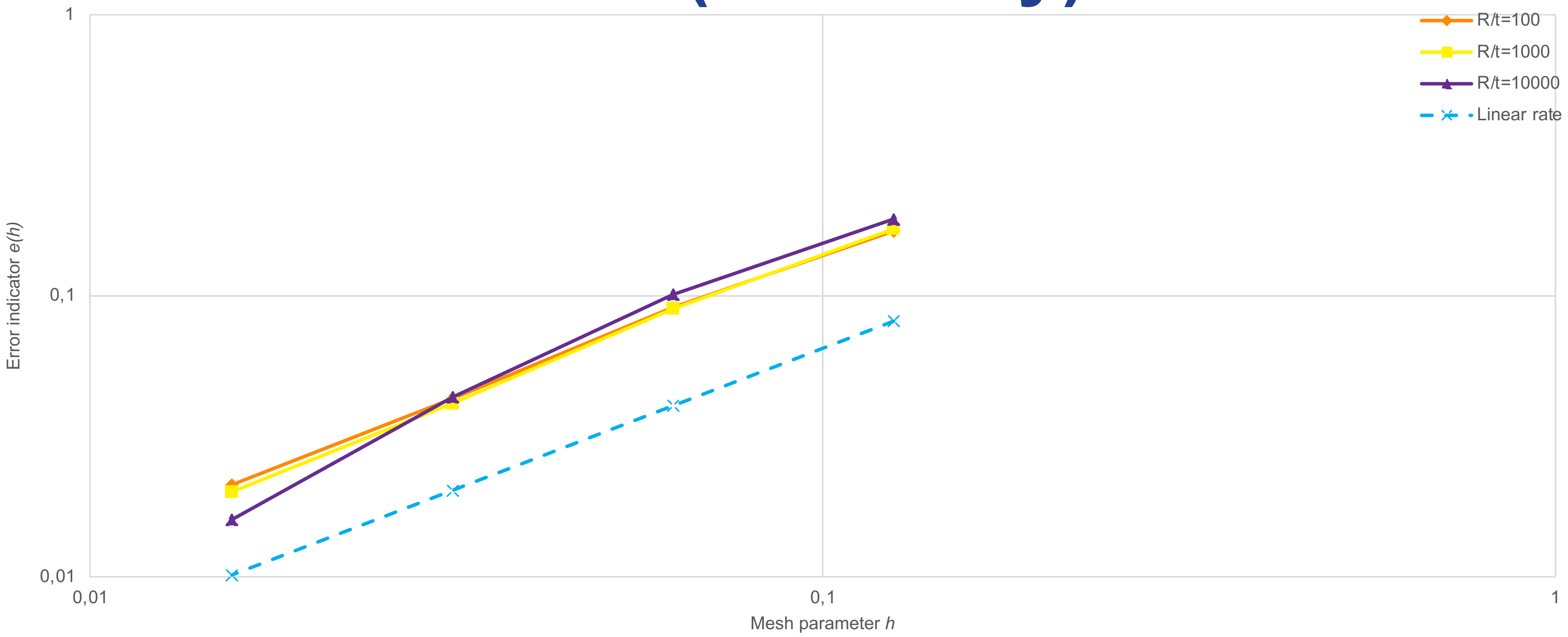

Doubly Curved Hyperboloid
Hiller and Bathe, COMPUT STRUCT 81

Same problem setup as before but the Gaussian curvature is not zero:

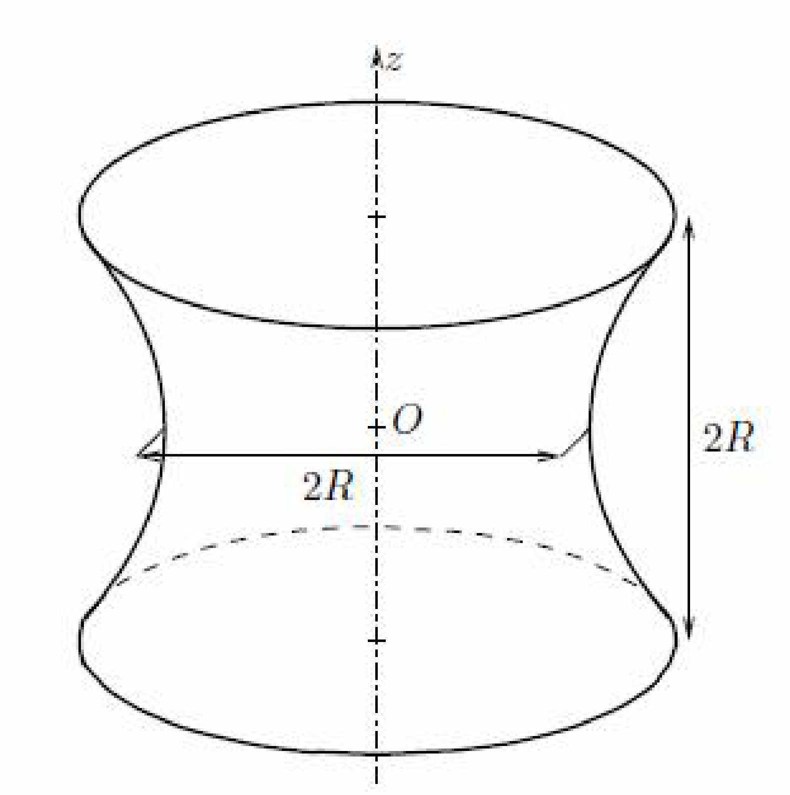

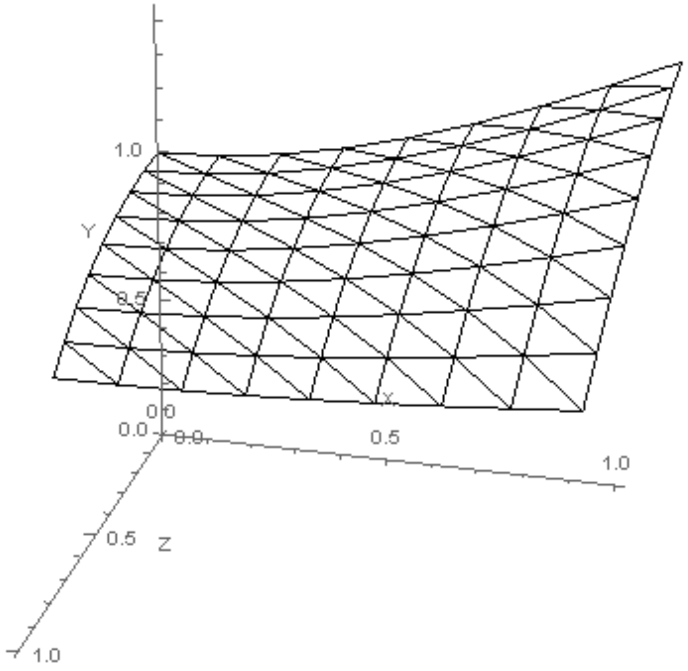

Hyperboloid with Free Ends (Bending) Stabilized MITC3S

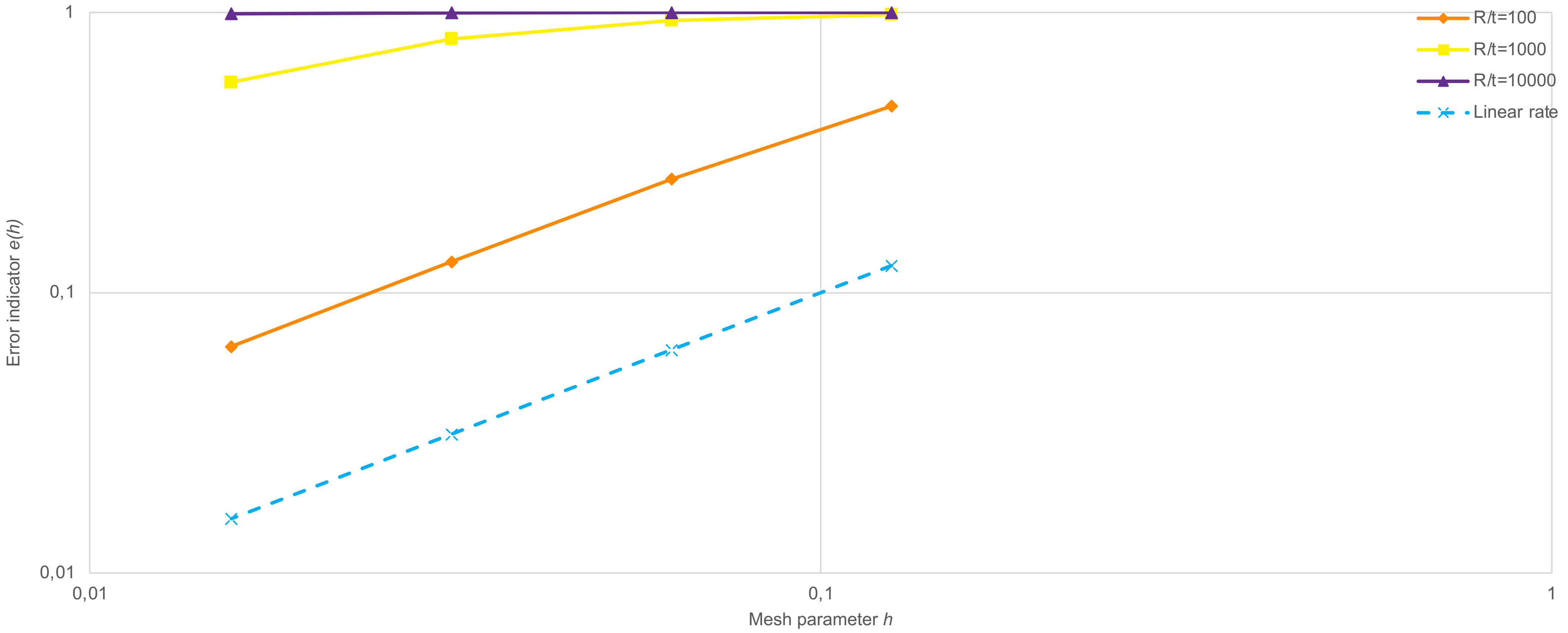

Hyperboloid with Free Ends (Bending) p=4

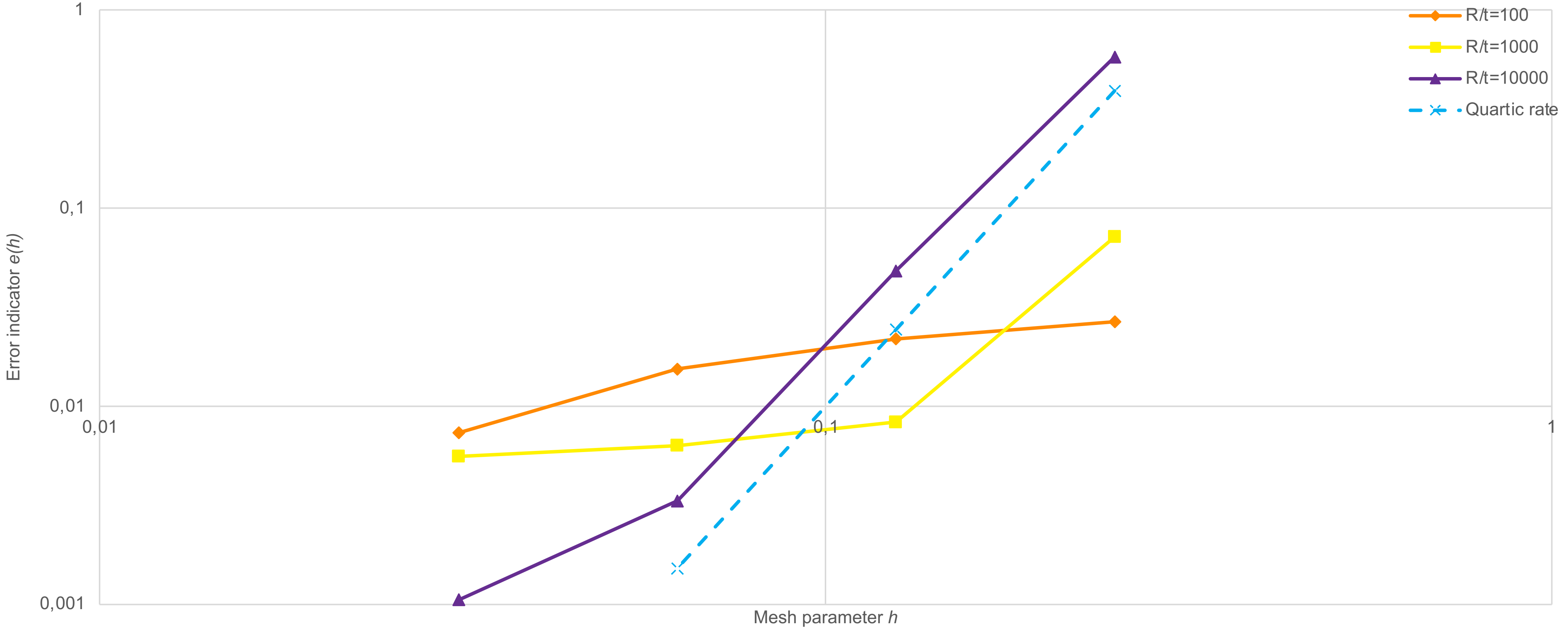

Pinched Cylinder

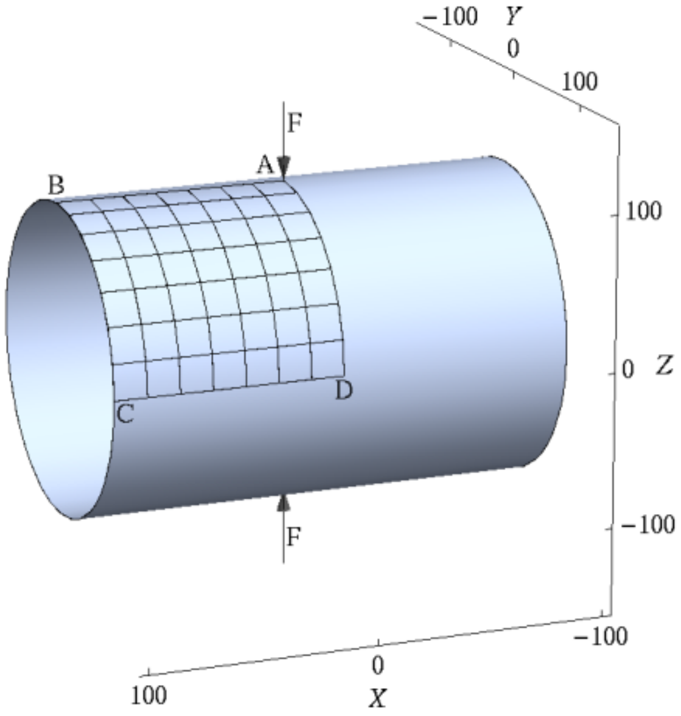

$$E = 3 \cdot 10^7, \quad \nu = 0.3, \quad \rho = 0.3$$

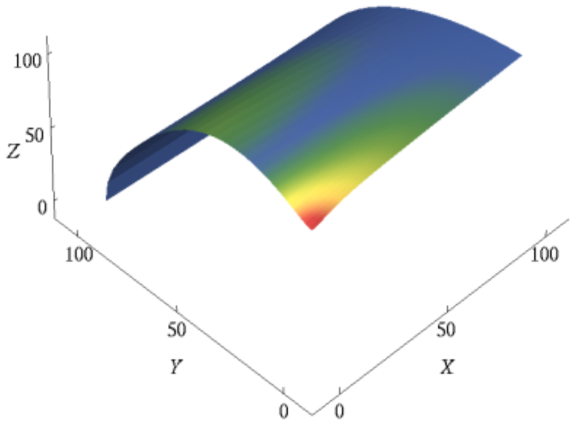

$R/t = 100$

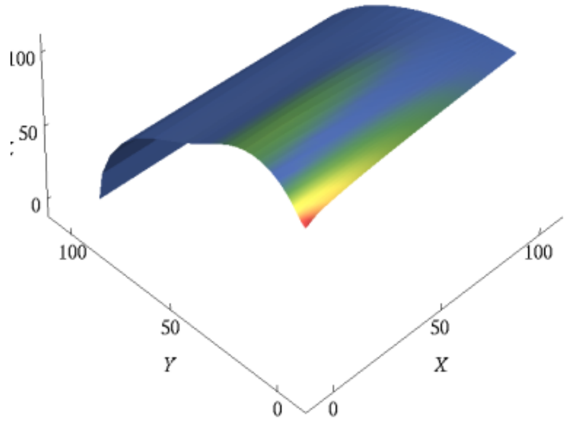

$R/t = 1000$

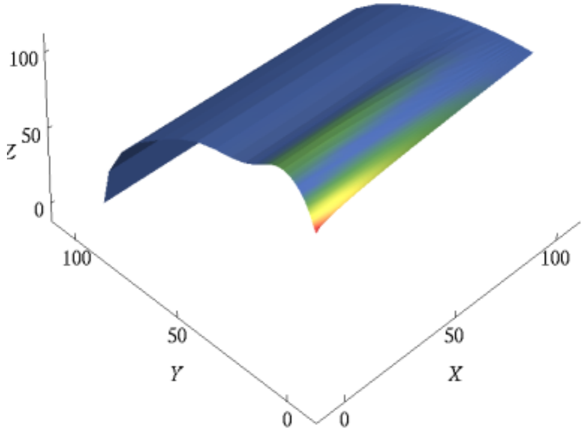

$R/t = 10000$

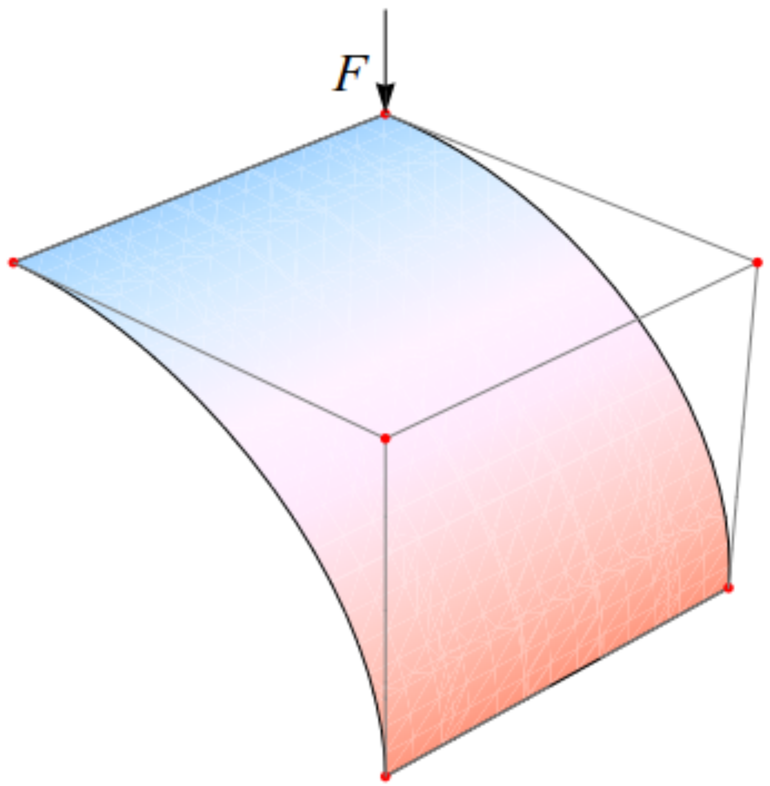

- The cylinder can be represented as a quadratic rational Bézier surface
- The FE space can be enriched by knot insertion and order elevation

Strain Energy Convergence, R/t=100

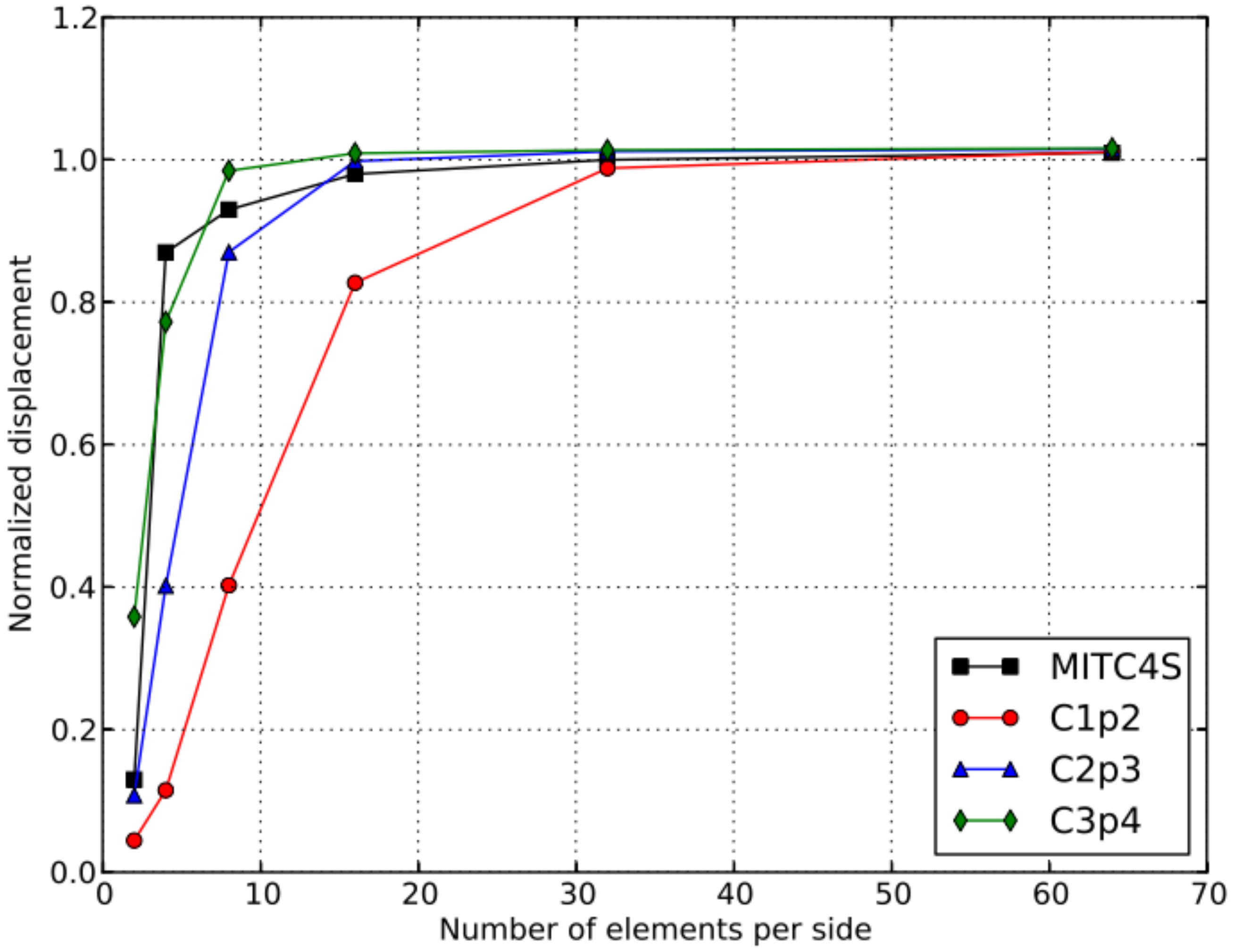

Strain Energy Convergence, R/t=1000

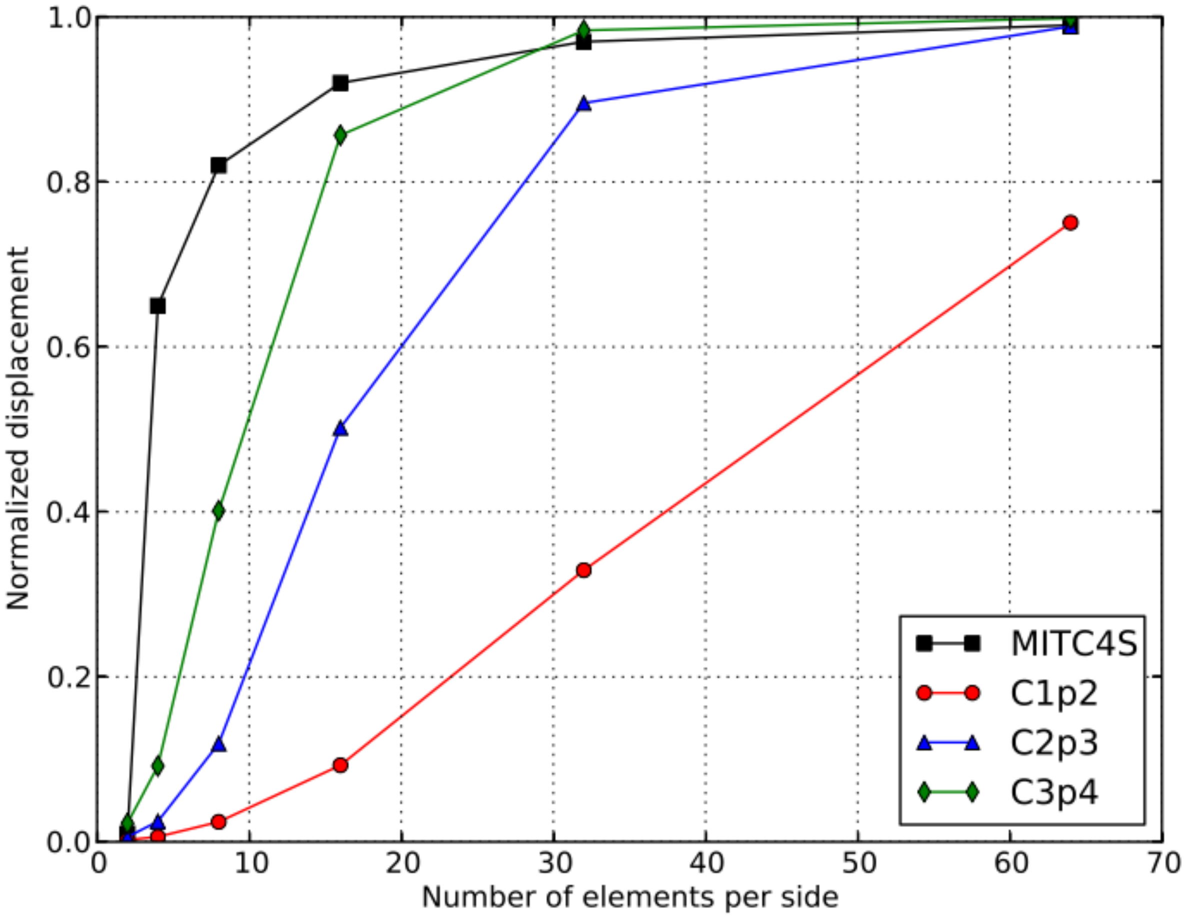

Buckling problem

Momentless pre-buckling state

The pre-buckling state is assumed to be characterized by membrane forces

$$N^0 = \begin{bmatrix} N^0_{xx} & N^0_{xy} \\ N^0_{xy} & N^0_{yy} \end{bmatrix}$$

Critical load

The limit of elastic stability $\lambda_b \in \mathbb{R}$ is defined as the minimum eigenvalue of the following problem:

Find $\lambda_b \in \mathbb{R}$ and $U \in \mathcal{U}$ $U \neq 0$ s.t.

$$A(U, V) = \lambda_b (N^0 \nabla w, \nabla \delta w)_{0,\Omega} \quad \forall V \in \mathcal{U}$$

Axially compressed cylinder

For a cylinder under uniform axial compression

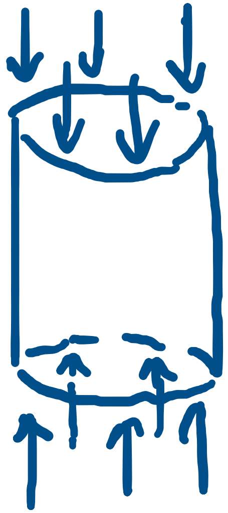

$$\lambda_b N^0 = \begin{bmatrix} Q & 0 \\ 0 & 0 \end{bmatrix}$$

where q is the critical load

Euler equation

Simplified shell equation for stability analysis:

$$\frac{Ed^3}{12(1-\nu^2)}\Delta^4 w + \frac{Ed}{R}\frac{\partial^4 w}{\partial x^4} + Q\,\Delta^2\left(\frac{\partial^2 w}{\partial x^2}\right) = 0$$

[Donnell – Mushtari – Vlasov – Pitkäranta theory]

Batdorf's buckling modes (1947)

Assume simple support and look for buckling modes of the form

1° $w(x,y) \sim \sin\left(\frac{m\pi x}{L}\right)$

2° $w(x,y) \sim \sin\left(\frac{m\pi x}{L}\right)\sin\left(\frac{ny}{R}\right)$

Axially symmetric modes

Defining $M = \frac{m\pi R}{L}$, we get

$$Q = \frac{Ed^3}{12(1-\nu^2)} \cdot \frac{M^2}{R^2} + \frac{Ed}{M^2}$$

and minimization w.r.t. M yields

$$M_b = \sqrt[4]{12(1-\nu^2)} \cdot \sqrt{\frac{R}{d}} \quad \& \quad Q_b = \frac{Ed^2}{\sqrt{3(1-\nu^2)}}$$

Angularly varying modes

Defining $N = \frac{nL}{\pi R}$, we get

$$Q \sim \frac{(m^2+N^2)^2}{m^2} + \frac{12 Z^2 m^2}{\pi^4 (m^2+N^2)^2} \; ; \quad Z = \frac{L^2}{Rd}\sqrt{1-\nu^2}$$

Minimization yields

$$N = \left\{ \frac{(12 Z^2)^{1/4}}{\pi} m - m^2 \right\}^{1/2} \quad \& \quad Q_b = \frac{Ed^2}{\sqrt{3(1-\nu^2)}}$$

Remarks about the buckling modes

- Both type of modes yield <u>the same critical load</u>

- The results are valid for moderately long cylinders $L > 1{,}69\sqrt{Rd}\,\sqrt[4]{1-\nu^2}$

FEM considerations

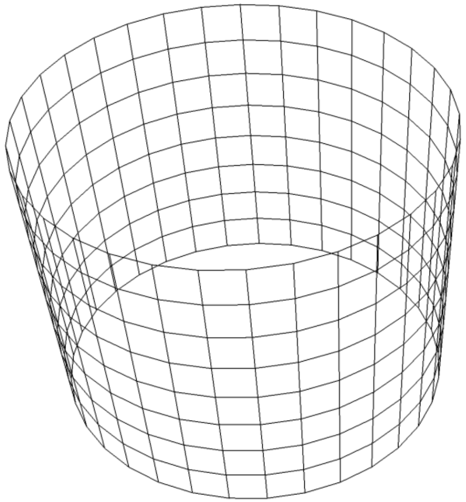

Dimensionless analysis

Assume: $L \sim R \sim 1$ (length unit)

Denote: $t = d/R$ (dimensionless thickness)

1° The number of axial waves is $m \sim \frac{1}{\sqrt{t}}$

2° The wave numbers are related by

$$n^2 \sim \frac{m}{\sqrt{t}} - m^2$$

Possible scales of the critical mode

1^0 $\quad l_x \sim t^{1/2} \qquad l_y \sim 1$

2^0 a) $\quad l_x \sim 1, \qquad l_y \sim t^{1/4}$

b) $\quad l_x \sim l_y \sim t^{1/2}$

Energy view of the buckling modes

Consider the simplified scaled energy density:

$$E(U) \doteq E_m(U) + E_s(U) + E_b(U)$$

$$= \|\beta_{xx}\|_{0,\Omega}^2 + \|\beta_{yy}\|_{0,\Omega}^2 + 4\|\beta_{12}\|_{0,\Omega}^2$$

$$+ \|\gamma_x\|_{0,\Omega}^2 + \|\gamma_y\|_{0,\Omega}^2$$

$$+ t^2\|\theta_{x,x}\|_{0,\Omega}^2 + t^2\|\theta_{y,y}\|_{0,\Omega}^2$$

Case 1

Displacement amplitudes:

$w \sim 1, \quad u_x \sim u_y \sim \theta_y \sim 0, \quad \theta_x \sim t^{-1/2}$

Scaled energy density:

$$\bar{E} \sim \|\theta_{x,x}\|_{0,\Omega}^2 + \|w\|_{0,\Omega}^2 + t^{-1}\|\theta_x + w_{,x}\|_{0,\Omega}^2$$

Timoshenko beam with effective thickness $t_{eff} = t^{1/2}$

Case 2 a)

Displacement scalings:

$$w \sim 1, \quad u_y \sim t^{1/4}, \quad u_x \sim t^{1/2}, \quad \theta_x \sim 1, \quad \theta_y \sim t^{-1/4}$$

Scaled energy density:

$$\bar{E} \sim t \|\theta_{x,x}\|_{0,\Omega}^2 + \|\theta_{y,y}\|_{0,\Omega}^2 + \|\beta_{xx}\|_{0,\Omega}^2$$

$$+ t^{-1} \|u_{y,y} + w\|_{0,\Omega}^2 + t^{-1/2} \|u_{x,y} + u_{y,x}\|_{0,\Omega}^2$$

$$+ t^{-1} \|\theta_x + w_{,x}\|_{0,\Omega}^2 + t^{-3/2} \|\theta_y + w_{,y}\|_{0,\Omega}^2$$

Case 2 b)

Displacement amplitudes:

$$w \sim 1, \quad u_x \sim u_y \sim t^{1/2}, \quad \theta_x \sim \theta_y \sim t^{-1/2}$$

Scaled energy density:

$$E \sim \|\theta_{x,x}\|_{0,\Omega}^2 + \|\theta_{y,y}\|_{0,\Omega}^2 + \|u_{x,x}\|_0^2 + \|u_{y,y} + w\|_{0,\Omega}^2$$
$$+ \|u_{x,y} + u_{y,x}\|_{0,\Omega}^2 + t^{-1}\|\theta_x + w_{,x}\|_{0,\Omega}^2 + t^{-1}\|\theta_y + w_{,y}\|_{0,\Omega}^2$$

Reissner-Mindlin plate with effective thickness $t_{eff} = t^{1/2}$

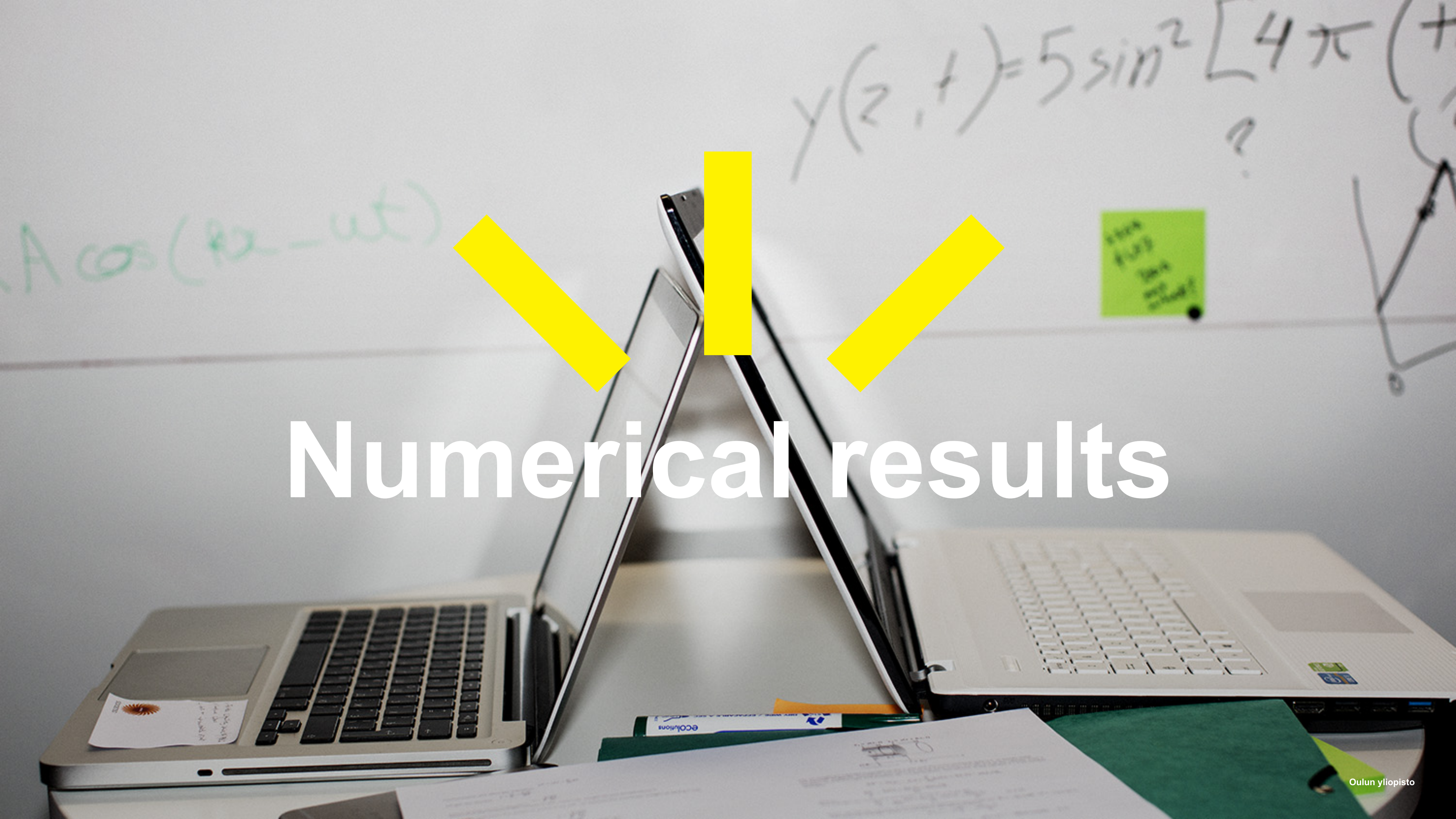

Numerical results

FE methods for RN

Standard isoparametric bilinear quad for $u_x, u_y, w, \theta_x, \theta_y$ (local formulation)

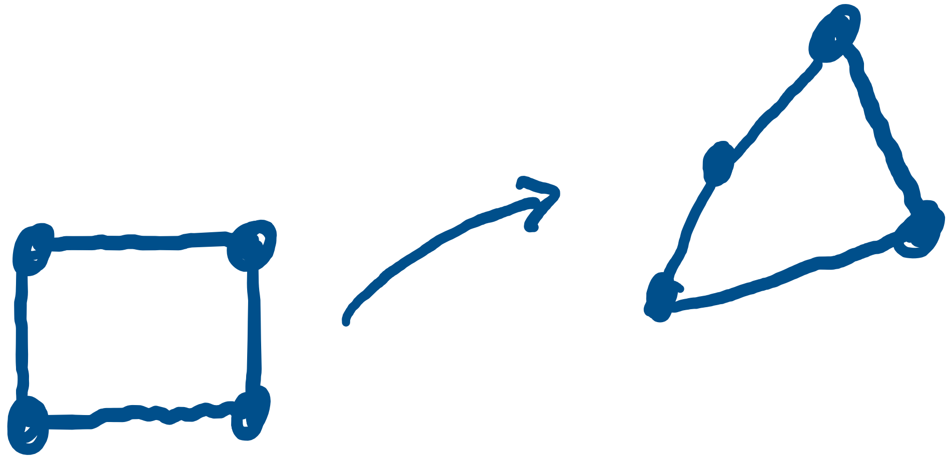

Alternative formulations

DISP4: no modifications

MITC4S: $\gamma \hookrightarrow R_h \gamma$, $\beta \hookrightarrow S_h \beta$

MITC4C: $\gamma \hookrightarrow R_h \gamma$

Buckling modes at *t*=0.005 (MITC4S)

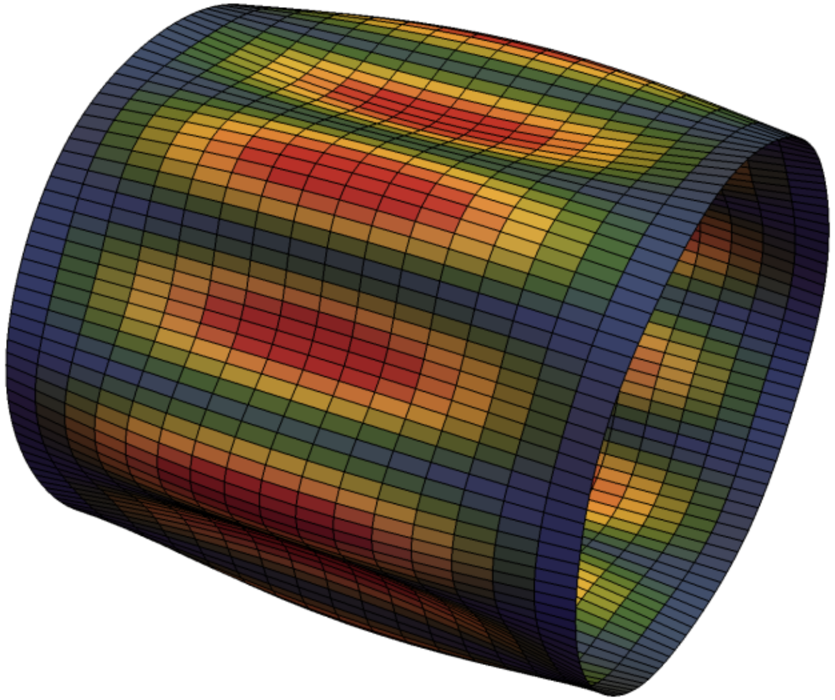

Case 2 a)

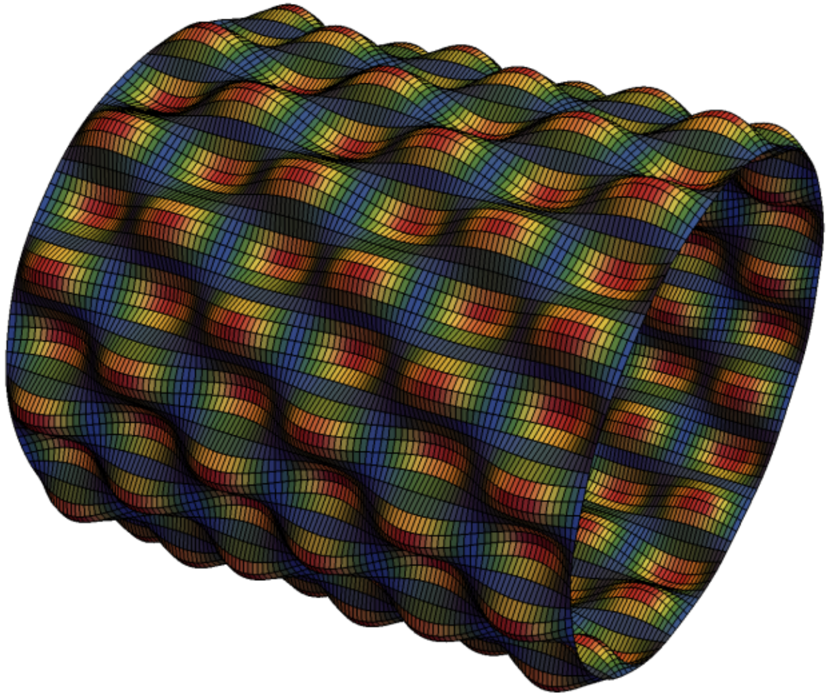

Case 2 b) ?

Convergence of the critical load

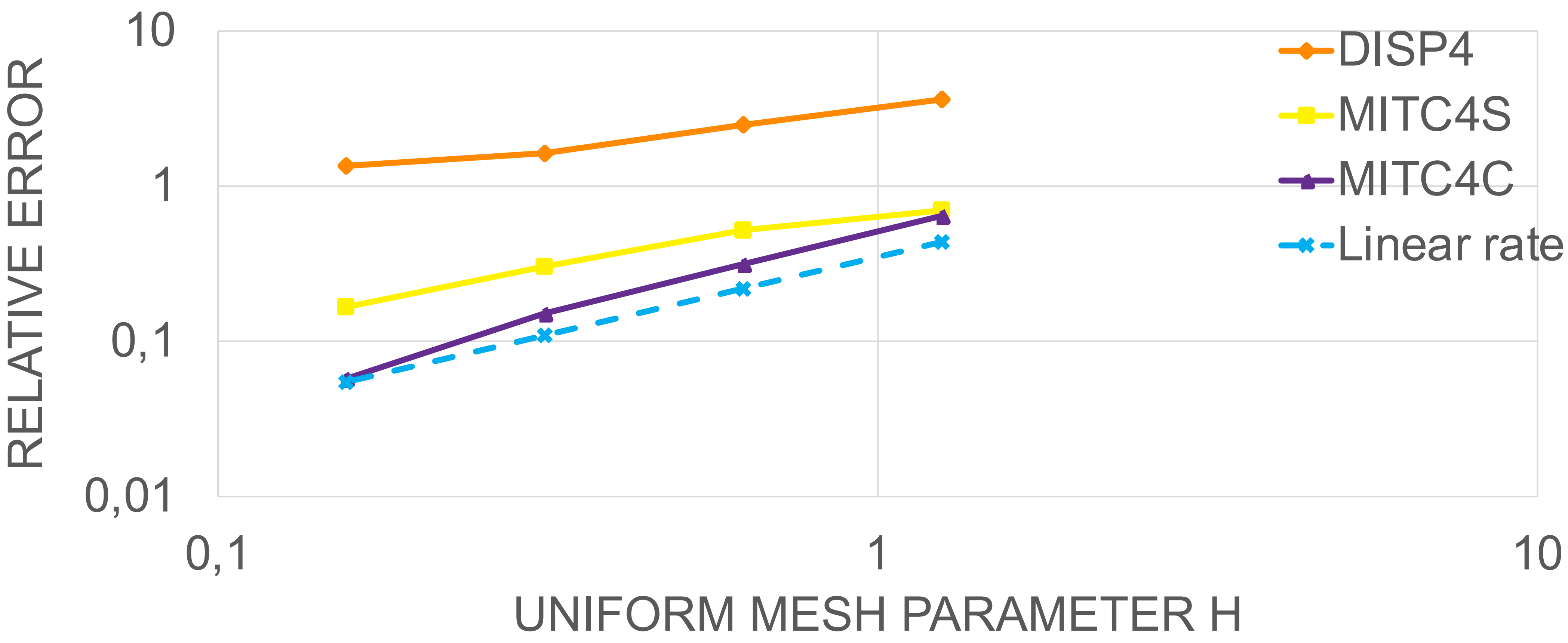

Convergence of the critical load (ii)

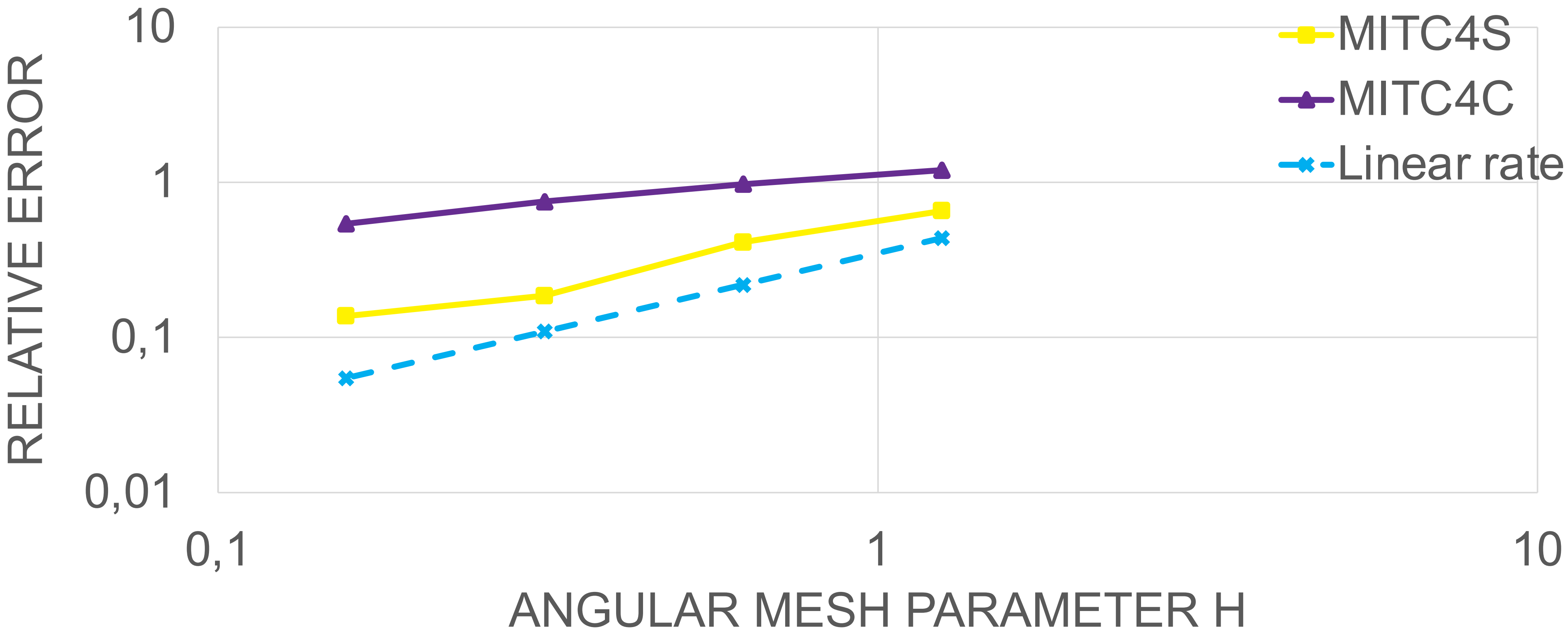

Concluding remarks

- The buckling modes fall into the intermediate category of shell deformations

- The buckling modes may vary in the length scales

$$L \sim t^{1/2} \quad \& \quad L \sim t^{1/4}$$

- The problems of transverse shear locking and membrane locking are present

References

Batdorf, S. B. (1947). A Simplified Method of Elastic-Stability Analysis for Thin Cylindrical Shells. *National Advisory Committee for Aeronautics*, *NACA-TR-87*.

Pitkäranta, J., Matache, A.-M., & Schwab, C. (2001). Fourier mode analysis of layers in shallow shell deformations. *Computer Methods in Applied Mechanics and Engineering*, *190*(22–23), 2943–2975.

Niemi, A. H. (2008). Approximation of shell layers using bilinear elements on anisotropically refined rectangular meshes. *Computer Methods in Applied Mechanics and Engineering*, *197*(45–48), 3964–3975.

Da Veiga, L. B., Hakula, H., & Pitkäranta, J. (2008). Asymptotic and numerical analysis of the eigenvalue problem for a clamped cylindrical shell. *Mathematical Models and Methods in Applied Sciences*, *18*(11), 1983–2002.

Lovadina, C., Mora, D., & Rodríguez, R. (2010). Approximation of the Buckling Problem for Reissner–Mindlin Plates. *SIAM Journal on Numerical Analysis*, *48*(2), 603–632.

References

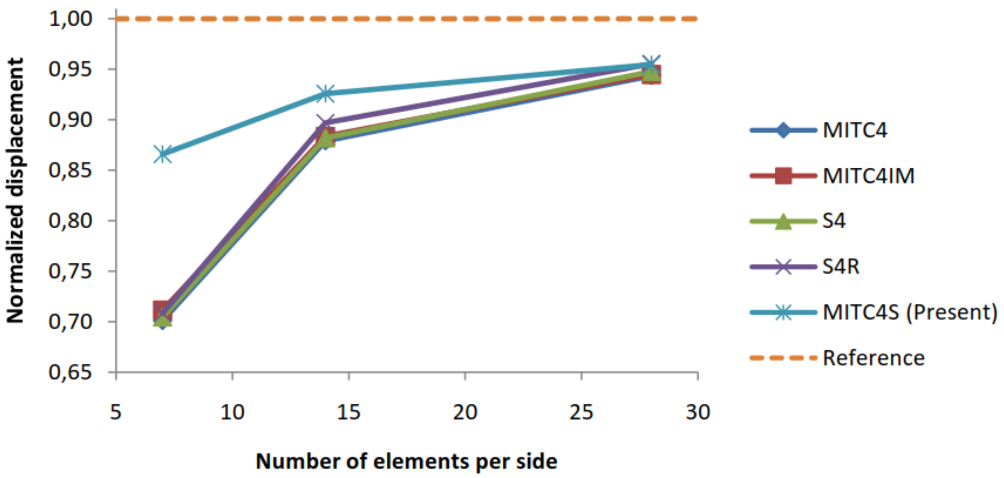

A.H. Niemi, "Benchmark Computations of Stresses in a Spherical Dome with Shell Finite Elements", SIAM J. Sci. Comput., Vol. 38, pp. B440-B457, (2016).

Antti H. Niemi.
A bilinear shell element based on a refined shallow shell model.
International Journal for Numerical Methods in Engineering, 81:485–512, 2010.

Antti H. Niemi, Ivo Babuška, Juhani Pitkäranta, and Leszek Demkowicz.
Finite element analysis of the Girkmann problem using the modern *hp*-version and the classical *h*-version.
Engineering with Computers, 28:123–134, 2011.

OULUN
YLIOPISTO